

# Excimer-pumped alkali vapor lasers: A new class of photoassociation lasers

J. D. Readle\*<sup>1</sup>, C. J. Wagner<sup>1</sup>, J. T. Verdeyen<sup>2</sup>, T. M. Spinka<sup>1</sup>, D. L. Carroll<sup>2</sup>, and J. G. Eden<sup>1</sup>

<sup>1</sup>Laboratory for Optical Physics and Engineering, Department of Electrical and Computer Engineering, University of Illinois, Urbana, IL 61801

<sup>2</sup>CU Aerospace, 2100 South Oak Street, Suite 206, Champaign, IL 61820

## ABSTRACT

Excimer-pumped alkali vapor lasers (XPALs) are a new class of photoassociation lasers which take advantage of the spectrally broad absorption profiles of alkali-rare gas collision pairs. In these systems, transient alkali-rare gas molecules are photopumped from the thermal continuum to a dissociative  $X^2\Sigma_{1/2}^+$  interaction potential, subsequently populating the  $n^2P_{3/2}$  state of the alkali. The absorption profiles  $\geq 5$  nm and quantum efficiencies  $>98\%$  have been observed in oscillator experiments, indicating XPAL compatibility with conventional high power laser diode arrays.

An alternative technique for populating the  $n^2P_{3/2}$  state is direct photoexcitation on the  $n^2P_{3/2} \leftarrow n^2S_{1/2}$  atomic transition. However, because the XPAL scheme employs an off-resonant optical pump, the strengths of resonantly-enhanced nonlinear processes are minimized. Additionally, the absorption coefficient may be adjusted by altering the number densities of the lasing species and/or perturbers, a valuable asset in the design of large volume, high power lasers.

We present an overview of XPAL lasers and their operation, including the characteristics of recently demonstrated systems photopumped with a pulsed dye laser. Lasing has been observed in Cs at both 894 nm and 852 nm by pumping CsAr or CsKr pairs as well as in Rb at 795 nm by pumping RbKr. These results highlight the important role of the perturbing species in determining the strength and position of the excimer absorption profile. It is expected that similar results may be obtained in other gas mixtures as similar collision pair characteristics have historically been observed in a wide variety of transient diatomic species.

**Keywords:** Laser, alkali, rare gas, excimer, exciplex, diode, satellite, XPAL

## 1. INTRODUCTION

A new class of photodissociation lasers have been demonstrated in which photoexcited alkali-rare gas collision pairs dissociate to produce inversion on an atomic alkali transition. These lasers provide pump acceptance linewidths broader than 5 nm and quantum efficiencies in excess of 98%. Because diode laser arrays typically have linewidths  $\sim 2$  nm, these characteristics make excimer-pumped alkali-vapor lasers (XPALs) promising candidates for diode laser-pumped systems capable of producing near-Gaussian beams ( $M^2$  approaching 1). XPAL pumping schemes have been realized in Cs-Ar-C<sub>2</sub>H<sub>6</sub>, Cs-Kr-C<sub>2</sub>H<sub>6</sub>, Cs-Ar and Rb-Kr-C<sub>2</sub>H<sub>6</sub> systems<sup>1-3</sup>, although the technique is by no means limited to alkali-rare gas combinations. The theory behind the operation of these lasers, together with their operating characteristics and future opportunities will be discussed.

\*jreadle@illinois.edu

## 2. SPECTROSCOPIC FOUNDATIONS

The photoassociation of alkali-rare gas collision pairs correspond to spectral satellites associated with atomic alkali resonance transitions<sup>4</sup>. Satellites may lie to either the blue or the red of the atomic transition they are associated with, and have been observed in both absorption and emission spectra of a wide variety of perturbed atomic species<sup>5</sup>. Satellites arise from a region of internuclear separation in which the interaction potentials of two molecular electronic states are approximately parallel. The key characteristic of these satellites which make them attractive for diode pumping is that they are often spectrally broad. For the blue satellites reported here, linewidths as large as 5 nm have been observed.

The XPAL scheme utilizes these satellites as a means by which excited atomic alkali states may be populated. This is illustrated in Fig. 1 for a Cs-Ar system where the interaction potentials have been adapted from Ref. 6. It is well known<sup>7</sup> that photoexcitation of CsAr collision pairs produce a well-defined, spectrally broad blue satellite corresponding to the  ${}^2P_{3/2} \rightarrow {}^2S_{1/2}$  ( $D_2$ ) line of Cs corresponding to a minima in the  $B^2\Sigma_{1/2}^+ - X^2\Sigma_{1/2}^+$  difference potential. Because the  $B^2\Sigma_{1/2}^+$  potential is repulsive, excimer pairs quickly dissociate to produce Cs ( $6p^2P_{3/2}$ ) + Ar ( $3p^6\ ^1S_0$ ). Inversion may then be obtained on the  $D_2$  transition, corresponding to four-level laser operation. Alternatively, by facilitating  ${}^2P_{3/2} \rightarrow {}^2P_{1/2}$  population relaxation, laser action on the  ${}^2P_{1/2} \rightarrow {}^2S_{1/2}$  ( $D_1$ ) transition at 894 nm can also be observed. This relaxation is often provided through collisions with a hydrocarbon. This pumping scheme corresponds to five-level operation.

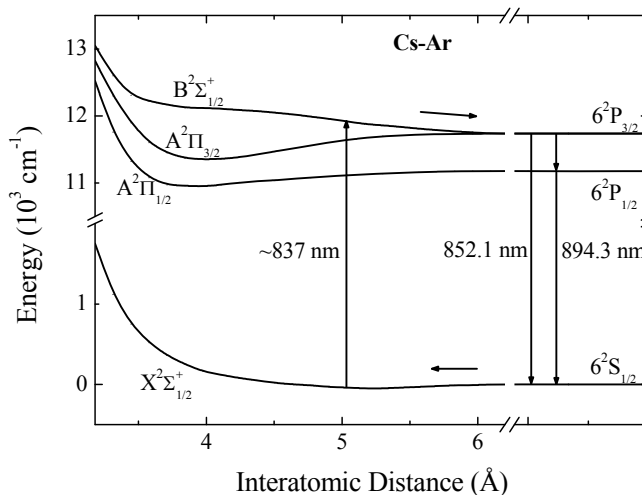


Figure 1. Interaction potentials of CsAr adapted from Ref. 6. The arrows indicate the various pumping pathways, with two different variations of the XPAL scheme shown. Laser action at 852.1 nm and 894.3 nm correspond to four- and five-level operation, respectively.

As mentioned previously, similar spectral satellites associated with a wide variety of atomic transitions have been reported over the past 80 years<sup>5</sup>. Tl is one such species, and schemes similar to those illustrated in Fig. 1 have been demonstrated in Tl mixtures. The first was in 1979, where Tl-Hg and Td-Cd-Ar satellites were photoexcited to produce laser action on the  $7^2S_{1/2} \rightarrow 6^2P_{3/2}$  Tl transition at 535.1 nm (cf. Ref. 8). Similar operation was later observed by Atamas *et al.* in a Tl-He mixture<sup>9</sup>. However, the XPAL scheme reported here has two unique characteristics compared to these earlier systems. First, the inverted alkali transitions all terminate on the ground state as opposed to an intermediate energy level. Also, in the case of four-level operation, there are *no intermediate states* involved. The implications of this characteristic will be discussed in further detail in Section 3.3.

Prior to the first XPAL demonstration, laser action on the  $D_1$  transition was obtained through direct photoexcitation of the atomic alkali species. This was reported in 2003, where an optical pump was tuned directly onto the  $D_2$  resonance of Rb<sup>10</sup>. In this laser,  ${}^2P_{3/2} \rightarrow {}^2P_{1/2}$  relaxation was provided by collisions with ethane ( $C_2H_6$ ). Similar three-level pumping schemes was later demonstrated in both Cs<sup>11</sup> and K<sup>12</sup>. The energy defect of the doublet ranges from  $57.7\text{ cm}^{-1}$  in K to  $554\text{ cm}^{-1}$  in Cs which correspond to quantum efficiencies  $>90\%$ . However, the  $D_2$  atomic transition is spectrally narrow ( $\sim 10\text{ GHz}$  with 1 atm of He buffer gas). This makes efficient coupling of semiconductor laser arrays having bandwidths on the order of 1 THz or 2 nm. Spectrally narrowing and frequency locking the output to match the atomic resonance is

both expensive and difficult, and is the primary reason that the highest power three-level system demonstrated to date has not exceeded 150 W (cf. Ref. 13). Also, it is important to recognize that laser action on the  $D_2$  line is *not possible* with direct  $^2P_{3/2} \leftarrow ^2S_{1/2}$  atomic photoexcitation as this would require inversion in a two-level system.

### 3. OSCILLATOR EXPERIMENTS

#### 3.1 Experimental setup

The setup used in the oscillator experiments described here is illustrated in Fig. 2. The second harmonic of an Nd:YAG was used to pump a tunable, pulsed dye laser and amplifiers capable of tuning over the range  $\sim 819\text{--}856$  nm with pulse energies approaching 2 mJ and pulse durations of approximately 4 ns. The dye laser serves as a surrogate for future diode pumping. The pump was delivered to the alkali laser cavity via a polarizing beamsplitter which also served to define the “L” shaped alkali laser cavity for perpendicularly polarized light. Cylindrical gas cells containing the alkali-rare gas mixtures were made of Pyrex and measured 10 cm long by 2.5 cm in diameter and had either plane-parallel or  $11^\circ$  angled windows. As seen in Fig. 2, this beamsplitter coupled with a broadband highly reflecting mirror ( $>99\%$ ) in order to provide a double-pass pump geometry in which unabsorbed pump radiation is ejected from the cavity. In the Cs experiments, both mirrors had a radius of curvature of 3 m and were separated by approximately 80 cm. A filter was utilized at the output of the laser cavity in order to eliminate any scattered pump light from entering the detector. Pulse energies were measured with carefully calibrated pyroelectric detectors and pulses were sampled both upon entering and exiting the alkali laser cavity via the polarizing beamsplitter. By recording all three of these energies, it is possible to determine the output energy as a function of energy absorbed in the gas cell.

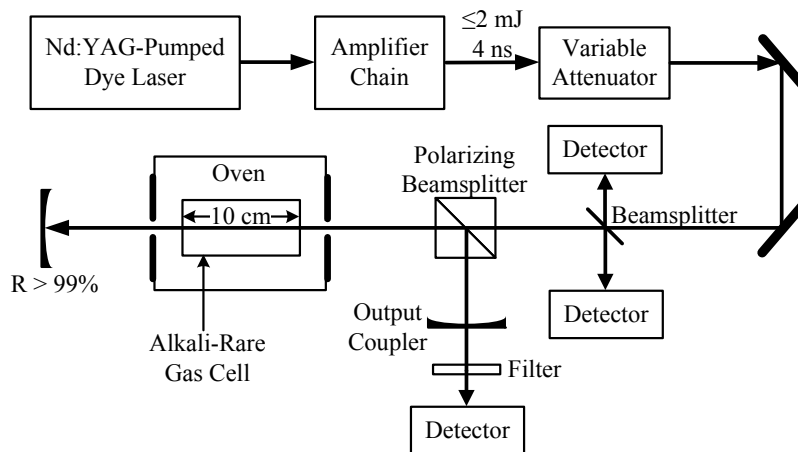


Figure 2. Experimental setup used in the oscillator experiments in which lasing was observed at both 894 nm ( $D_1$ ) and 852 nm ( $D_2$ ) transitions in Cs and 794 nm ( $D_1$ ) transition in Rb.

#### 3.2 Five-level operation employing collisional relaxant

The first experimental demonstrations of an XPAL laser<sup>1,2</sup> occurred in a mixture containing natural abundance Cs,  $[\text{Ar}] = 1.6 \cdot 10^{19} \text{ cm}^{-3}$ , and  $[\text{C}_2\text{H}_6] = 3.2 \cdot 10^{18} \text{ cm}^{-3}$ . The presence of  $\text{C}_2\text{H}_6$  promoted laser action at 894 nm, corresponding to five-level operation. Figure 2 shows excitation spectra obtained in the Cs-Ar- $\text{C}_2\text{H}_6$  mixture in which each point corresponds to the output pulse energy normalized to the input pulse energy as a function of dye laser wavelength. This was done in order to account for the variation in dye pulse energy pump wavelength ( $\lambda_p$ ). Data are shown for temperatures of 410 K, 434 K, and 450 K (corresponding to  $[\text{Cs}] = 1.2 \cdot 10^{14} \text{ cm}^{-3}$ ,  $3.6 \cdot 10^{14} \text{ cm}^{-3}$ , and  $7.2 \cdot 10^{14} \text{ cm}^{-3}$ , respectively). It should be noted that the ordinate is on a logarithmic scale and the absorption spectra obtained at 471 K is plotted in order to illustrate the expected symmetry in absorption and excitation. At each of the three excitation temperatures plotted, the spectral breadth of the blue satellite is  $\geq 5$  nm and the peak intensity increases approximately linearly with  $[\text{Cs}]$ . As indicated by the upper x-axis, photoexcitation of the blue satellite corresponds to

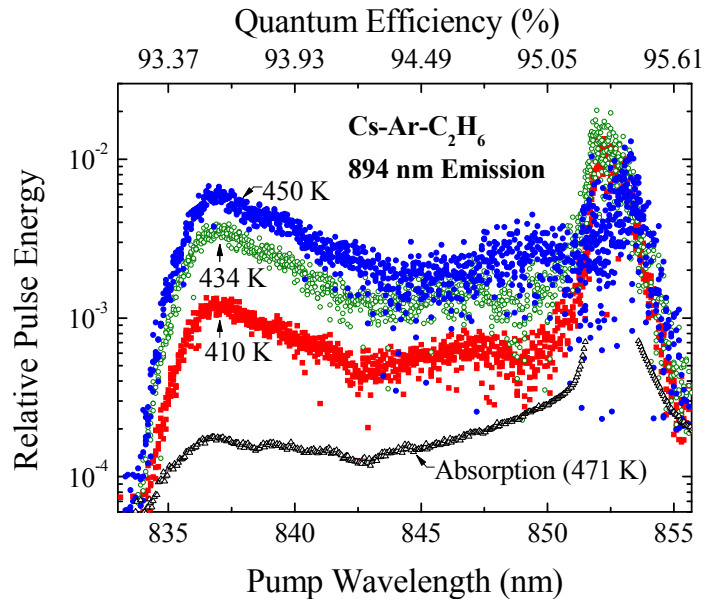


Figure 3. Excitation spectra obtained for a Cs-Ar-C<sub>2</sub>H<sub>6</sub> mixture in which the relative output pulse energy at 894 nm was monitored as a function of dye laser pump wavelength and normalized to the incident pump energy. The filled red squares correspond to a gas cell temperature of 410 K ([Cs] = 1.2 · 10<sup>14</sup> cm<sup>-3</sup>), the open green circles to 434 K ([Cs] = 3.6 · 10<sup>14</sup> cm<sup>-3</sup>) and the filled blue circles to 450 K ([Cs] = 7.2 · 10<sup>14</sup> cm<sup>-3</sup>). The absorption spectrum (open black triangles) at 471 K is provided for comparison, with the region near 852 nm omitted for clarity.

quantum efficiencies >93%. Pumping at ~852 nm corresponds to direct atomic excitation on the D<sub>2</sub> transition, and the degradation of this spectral peak at higher values of [Cs] is attributed to the increased frequency of undesired nonlinear processes, including parasitic oscillations between the cell windows and multi-photon ionization.

As Fig. 3 indicates, the blue satellite provides over twice the required spectral bandwidth for commercial laser diode arrays having nominal linewidths of 2 nm. This offers a significant advantage over three-level operation, at the cost of an approximately 2% reduction in the quantum efficiency. Also indicated by Fig. 2, the absorption coefficient of the satellite is smaller than that on the atomic resonance. Nevertheless, on a per-photon-absorbed basis, the threshold and efficiency of the laser are identical (within experimental uncertainty) when pumping on the peak of the satellite at 836.7 nm versus directly photoexciting the D<sub>2</sub> transition at 852.1 nm. The energy out (E<sub>o</sub>) at 894 nm as a function of energy absorbed (E<sub>a</sub>) is depicted in Fig. 4 for a gas cell temperature of 435 K, corresponding to [Cs] = 3.8 · 10<sup>14</sup> cm<sup>-3</sup>. For both pump wavelengths, the threshold is approximately 50 μJ. The overlapping data of Fig. 4 indicates that, assuming a cavity design that allows for all incident photons to be absorbed, there is no efficiency loss associated with a smaller absorption coefficient. In fact, far from serving as a liability, a smaller absorption coefficient may prove incredibly valuable due to the reduction in the complexity of the design of a radially-pumped gas cell. Excessive absorption degrades the spatial uniformity of the gain profile by providing greater gain near the gas cell walls than at the center.

Following this success in photoexciting Cs-Ar pairs, a similar system was realized in a Cs-Kr-C<sub>2</sub>H<sub>6</sub> mixture<sup>3</sup>. As one expected, the increased polarizability of Kr over Ar causes the Cs-Kr interaction potentials to differ from those of Cs-Ar. Differences in the X<sup>2</sup>Σ<sub>1/2</sub><sup>+</sup> and B<sup>2</sup>Σ<sub>1/2</sub><sup>+</sup> potentials result in a shift in the peak wavelength of the satellite from 836.7 nm in CsAr to 841.1 nm in CsKr and decrease its spectral breadth (≥5 nm in CsAr<sup>2</sup> and ≥2 nm in CsKr<sup>3</sup>). This spectral shift corresponds to a slight increase in the quantum efficiency of ~0.5% to 94.1%. These characteristics are depicted in Fig. 5 which compares the excitation spectra for 894 nm emission in both Cs-Ar and Cs-Kr mixtures. Note that the spectra have each been normalized to ~1 for clarity.

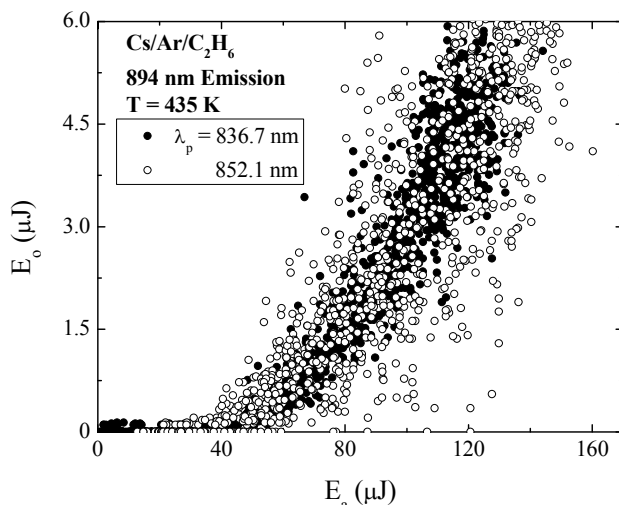


Figure 4. Energy out ( $E_o$ ) as a function of energy absorbed ( $E_a$ ) for 894 nm emission from a Cs-Ar-C<sub>2</sub>H<sub>6</sub> mixture. The filled circles correspond to a pump wavelength of 836.7 nm and the open circles to 852.1 nm. At 435 K,  $[Cs] = 3.8 \cdot 10^{14} \text{ cm}^{-3}$ .

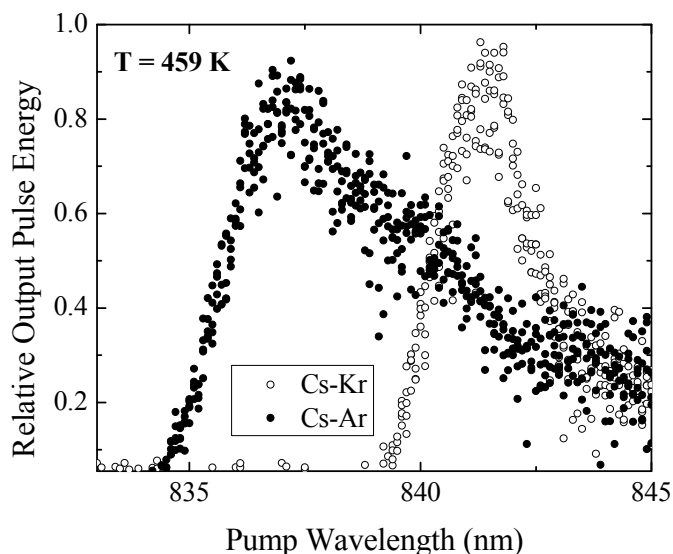


Figure 5. Comparison of normalized excitation spectra for 894 nm emission from Cs-Ar-C<sub>2</sub>H<sub>6</sub> and Cs-Kr-C<sub>2</sub>H<sub>6</sub> mixtures. Note that the Cs-Ar satellite (filled circles) peaks at  $\sim 836.7$  nm while the Cs-Kr satellite peaks at  $\sim 841.1$  nm. At 459 K,  $[Cs] = 1.0 \cdot 10^{15} \text{ cm}^{-3}$ .

Unique behavior observed in the Cs-Kr-C<sub>2</sub>H<sub>6</sub> mixture absent in Cs-Ar-C<sub>2</sub>H<sub>6</sub> is apparent in Fig. 6 which displays the laser pulse energy as a function of absorbed energy for both three- and five-level operation at a temperature of 458 K (corresponding to  $[Cs] = 1.0 \cdot 10^{15} \text{ cm}^{-3}$ ). In contrast to Fig. 4, pumping into the blue satellite in this manner leads to *improved* threshold and slope efficiency over direct atomic photoexcitation. The threshold energy is  $\sim 85 \mu\text{J}$  under at 841.1 nm photoexcitation compared to  $\sim 120 \mu\text{J}$  with 852.1 pumping, corresponding to a decrease of  $\sim 30\%$ . Slightly above threshold, the slope efficiencies are  $(3.3 \pm 1.1)\%$  for 841 nm pumping and  $(2.4 \pm 0.6)\%$  for 852 nm pumping, corresponding to an approximate average slope efficiency increase of  $\geq 30\%$ . This performance enhancement is attributed to a decrease in parasitic nonlinear effects resulting from having the pump tuned off of the atomic resonance. The departure from the nearly overlapping traces observed in Fig. 4 serves to further illustrate the dependence of laser performance on the interactions of the lasing and perturber species.

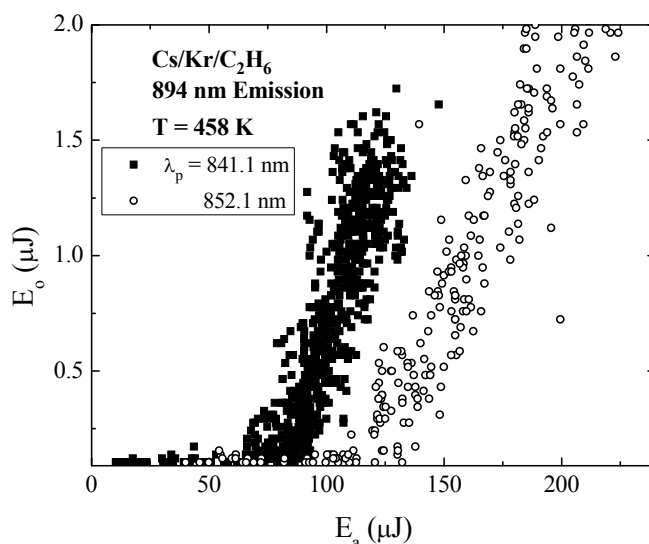


Figure 6. Laser energy out ( $E_o$ ) as a function of energy absorbed ( $E_a$ ) for 894 nm emission from a Cs-Kr- $C_2H_6$  mixture. The black squares correspond to a pump wavelength of 841.1 nm and the open circles to 852.1 nm. At 458 K,  $[Cs] = 1.0 \cdot 10^{15} \text{ cm}^{-3}$ .

In addition to the Cs XPALs that have been demonstrated, five-level laser operation on the  $D_1$  line of Rb at 794 nm has been observed in a gas mixture consisting of Rb,  $[Kr] = 1.6 \cdot 10^{19} \text{ cm}^{-3}$ , and  $[C_2H_6] = 3.2 \cdot 10^{18} \text{ cm}^{-3}$ . The blue satellite in this gas mixture peaks at  $\sim 760 \text{ nm}$ , corresponding to a quantum efficiency of 95.7%. This result serves to verify the hypothesis that XPAL operation may be realized in a variety of lasant species. An immediate implication of this confirmation is that there is significant flexibility in engineering the absorption and emission spectra in order to best match the desired characteristics of the laser output or pumping source.

### 3.3 Four-level operation without intermediate states

As discussed previously, it is possible to obtain inversion on the  $D_2$  transition by pumping a blue satellite and restricting the rate of  $^2P_{3/2} \rightarrow ^2P_{1/2}$  population transfer. In the experiments described here, this was accomplished by preparing a gas cell containing only Cs and Ar. As in the five-level experiments,  $[Ar] = 1.6 \cdot 10^{19} \text{ cm}^{-3}$ . An immediate advantage of this version of the XPAL pumping scheme is the  $\sim 4\%$  increase in quantum efficiency it provides in Cs over five-level operation, increasing it from  $>93\%$  to  $>98\%$ . Additionally, with the exception of K-He (cf. Ref. 14), all of the demonstrations of three- and five-level alkali lasers to date have relied on hydrocarbons to provide the requisite relaxation. Hydrocarbons in the presence of an alkali will degrade over time to produce alkali-hydrides and carbon “soot” which deposits on the cell windows, significantly reducing laser efficiency<sup>14</sup>. Finally, it should be reiterated that  $D_2$  laser action is *not possible* through direct photoexcitation of the same atomic resonance.

In addition to these operational advantages, four-level operation illustrates interesting characteristics of the collisionally-coupled states. At the temperatures of interest ( $\sim 400\text{-}500 \text{ K}$ ), the association and dissociation rates of the alkali-rare gas collision-pairs are on the order of tens to hundreds of ps. With such fast population transfer, one might argue that the population in  $^2S_{1/2}$  and  $X^2\Sigma_{1/2}^+$  states can be approximately related to one another by a scalar constant. Similarly, the  $^2P_{3/2}$  and  $B^2\Sigma_{1/2}^+$  states would be coupled by a slightly different scalar constant. This would indicate that the rate equations, which would normally be written for four distinct states for four-level operation, could now be written in only two equations through simple substitution. However, were this the case, one would conclude that laser action is not possible. Since these experiments have demonstrated this conclusion to be incorrect, they highlight importance of considering collision-pair contributions beyond the effects of simple collisional broadening.

Figure 7 shows the excitation spectra for emission at 852 nm obtained in a mixture containing Cs and  $[Ar] = 1.6 \cdot 10^{19} \text{ cm}^{-3}$ . Spectra are plotted at temperatures of 464 K, 475 K and 485 K (corresponding to  $[Cs]$  values of  $1.3 \cdot 10^{15} \text{ cm}^{-3}$ ,  $1.9 \cdot 10^{15} \text{ cm}^{-3}$  and  $2.8 \cdot 10^{15} \text{ cm}^{-3}$ , respectively). Just as in Fig. 3, the output energy was normalized to the input energy, although in Fig. 7 each data point corresponds to the average of four such measurements. Just as in the

five-level experiments, the blue satellite provides a spectrally broad pump acceptance region which in these experiments is observed to be  $\geq 3$  nm. The pump acceptance bandwidth reduction when compared with that observed in Fig. 3 is attributed primarily to the increased degeneracy of the  $^2P_{3/2}$  state ( $g = 4$ ) over that of  $^2P_{1/2}$  state ( $g = 2$ ), although differences in mirror reflectivities are also believed to play a role. The upper x-axis of Fig. 7 indicates the quantum efficiency as a function of pump wavelength, showing that values  $>98\%$  are obtained when pumping into the blue satellite region ( $\sim 835.5 \text{ nm} \leq \lambda_p \leq \sim 838.5 \text{ nm}$ ).

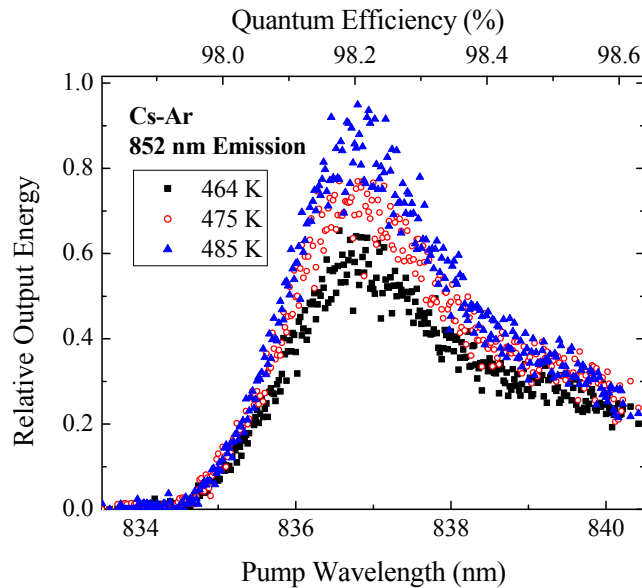


Figure 7. Excitation spectra obtained for 852 nm emission from a Cs-Ar mixture in which the relative output pulse energy was monitored as function of dye laser pump wavelength. The black squares correspond to  $T = 464 \text{ K}$  ( $[\text{Cs}] = 1.3 \cdot 10^{15} \text{ cm}^{-3}$ ), the open red circles to  $475 \text{ K}$  ( $[\text{Cs}] = 1.9 \cdot 10^{15} \text{ cm}^{-3}$ ) and the blue triangles to  $485 \text{ K}$  ( $[\text{Cs}] = 2.8 \cdot 10^{15} \text{ cm}^{-3}$ ).

The dependence of the alkali laser output energy on the pump energy absorbed at temperatures  $464 \text{ K}$ ,  $474 \text{ K}$  and  $485 \text{ K}$  (corresponding to  $[\text{Cs}]$  values of  $1.3 \cdot 10^{15} \text{ cm}^{-3}$ ,  $1.9 \cdot 10^{15} \text{ cm}^{-3}$  and  $2.8 \cdot 10^{15} \text{ cm}^{-3}$ , respectively) for a fixed pump wavelength of  $836.7 \text{ nm}$  corresponding to the peak of the blue satellite is depicted in Fig. 8. The observed threshold energies of  $130 \mu\text{J}$ ,  $175 \mu\text{J}$  and  $250 \mu\text{J}$  increase approximately linearly with  $[\text{Cs}]$  as is expected for a lasing transition which terminates on the ground state. At a fixed temperature, the slope efficiency increases with absorbed energy. Additionally, the slope efficiency appears to decrease with increasing gas cell temperature. These characteristics are not yet well understood, although they are consistent with similar data observed for five-level operation in Cs-Kr- $\text{C}_2\text{H}_6$  (cf. Ref. 3).

We believe that, by pumping into the red satellite of the  $D_2$  line quantum efficiencies  $>100\%$  may be obtained. For CsKr, the red satellite peaks at approximately  $853 \text{ nm}$ , manifesting as a strong asymmetry to the red of the  $D_2$  line center. By pumping a system in this manner, it should be possible for small amounts of energy (on the order of tens of  $\text{cm}^{-1}$  per photon) from the thermal bath to be transferred to the atomic alkali species as the excimer dissociates. This would effectively *cool* the gas medium during laser operation, a valuable characteristic for systems in which excess heat degrades system performance by lowering efficiency or reducing beam quality. Work to realize an XPAL laser with over  $100\%$  quantum efficiency in this manner is currently underway.

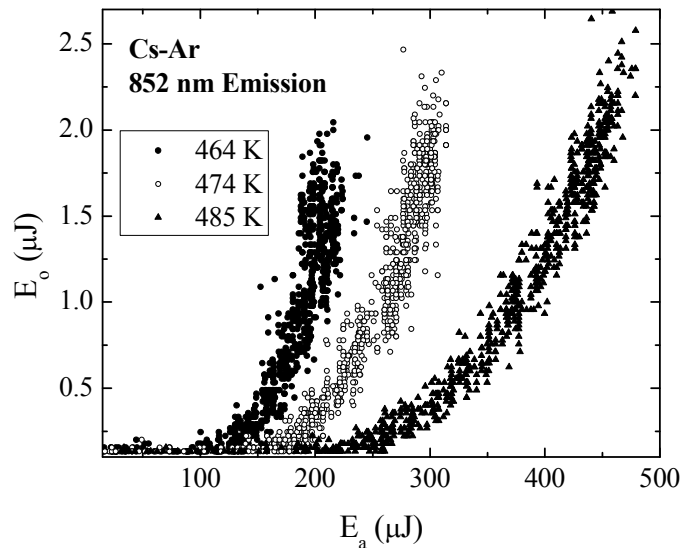


Figure 8. Laser output energy ( $E_o$ ) at 852 nm as a function of pump energy absorbed ( $E_a$ ) in a Cs-Ar mixture for a pump wavelength of 836.7 nm. Data for gas cell temperatures of 464 K (filled circles;  $[Cs] = 1.3 \cdot 10^{15} \text{ cm}^{-3}$ ), 474 K (open circles;  $[Cs] = 1.9 \cdot 10^{15} \text{ cm}^{-3}$ ) and 485 K (filled triangles;  $[Cs] = 2.8 \cdot 10^{15} \text{ cm}^{-3}$ ) are shown.

#### 4. CONCLUSION

The XPALs demonstrated to date are the first members of a new class of photodissociation lasers in which transient alkali-rare gas molecules provide an efficient and spectrally broad optical pumping pathway for obtaining inversion on an alkali transition. Both four- and five-level laser schemes have been presented, with spectral breadths larger than 5 nm and quantum efficiencies above 98% observed. These characteristics make XPAL systems well-suited for pumping with high power laser diode arrays. Additionally, in the case of four-level operation, a collisional relaxant species is no longer required. Although these early successes have been limited to Cs and Rb, we see no obstacles preventing realization of the XPAL scheme in the other alkalis including Li and Na. Extension of the excimer pumping scheme is not limited to alkali-rare gas combinations as illustrated by previous work in Tl gas mixtures, highlighting the potential for future adaptations of this technique to provide new and unique opportunities in the field of optically-pumped gas lasers.

#### ACKNOWLEDGEMENTS

Support of this work by the U.S. Air Force Office of Scientific Research under Grant Nos. FA9550-07-1-0575 and AF FA9550-07-1-0003 are gratefully acknowledged.

#### REFERENCES

- [1] Readle, J. D., Wagner, C. J., Verdeyen, J. T., Carroll, D. L. and Eden, J. G., "Lasing in Cs at 894.3 nm pumped by the dissociation of CsAr excimers", *Electron. Lett.*, 44, 1466-1467 (2008).
- [2] Readle, J. D., Wagner, C. J., Verdeyen, J. T., Spinka, T. M., Carroll, D. L. and Eden, J. G., "Pumping of atomic alkali lasers by photoexcitation of a resonance line blue satellite and alkali-rare gas excimer dissociation," *Appl. Phys. Lett.*, 94, 251112-1-251112-3 (2009).
- [3] Readle, J. D., Verdeyen, J. T., Eden, J. G., Davis, S. J., Gabally-Kinney, K. L., Rawlins, W. T. and Kessler, W. J., "Cs 894.3 nm laser pumped by photoassociation of Cs-Kr pairs: excitation of the Cs D<sub>2</sub> blue and red satellites," *Opt. Lett.*, 34, 3638-3640 (2009).

- [4] Hedges, R. E. M., Drummond, D. L. and Gallagher, A., "Extreme-wing line broadening and Cs-inert-gas potentials," *Phys. Rev. A*, 6, 1519-1544 (1972).
- [5] Ch'en, S. -Y. and Takeo, M., "Broadening and shift of spectral lines due to the presence of foreign gases," *Rev. Mod. Phys.*, 29, 20-73 (1957).
- [6] Chen, C. L. and Phelps, A. V., "Absorption coefficients for the wings of the first two resonance doublets of cesium broadened by argon," *Phys. Rev. A.*, 7, 470-479 (1973).
- [7] Pascale, J. and Vandeplanque, J., "Excited molecular terms of the alkali-rare gas atom pairs," *J. Chem. Phys.*, 60, 2278-2289 (1974).
- [8] Chilukuri, S., "Selective optical excitation and inversions via the excimer channel: Superradiance at the thallium green line," *App. Phys. Lett.*, 34, 284-286 (1979).
- [9] Atamas, S. N., Bukshpun, L. M., Koptev, I. V., Latush, E. L. and Sém, M. F., "Stimulated emission of the 535 nm thallium line as a result of quiresonant optical pumping of a Tl-He mixture by radiation from a recombination He-Ca laser," *Sov. J. Quant. Electron.*, 11, 229-231 (1984).
- [10] Krupke, W. F., Beach, R. J., Kanz, V.K. and Payne, S.A., "Resonance transition 795-nm rubidium laser," *Opt. Lett.*, 28, 2336-2338 (2003).
- [11] Beach, R. J., Krupke, W. F., Kanz, V. K., Payne, S.A., Dubinskii, M. A. and Merkle, L.D., "End-pumped continuous-wave alkali vapor lasers: experiment, model, and power scaling," *J. Opt. Soc. Am. B*, 21, 2151-2163 (2004).
- [12] Zhdanov, B., Maes, C., Ehrenreich, T., Havko, A., Koval, N., Meeker, T., Worker, B., Flusche, B. and Knize, R. J., "Optically pumped potassium laser," *Opt. Commun.*, 270, 353-355 (2007).
- [13] Zweiback, J. and Krupke B., "Rubidium and potassium alkali lasers," *Proc. SPIE 7196*, 71960E-1-71960E-5 (2009).
- [14] Zhdanov, B. V. and Knize, R. J., "Hydrocarbon-free potassium laser," *Electron. Lett.*, 43, 1024-1025 (2007).